Enhanced Dynamic Performance of Quantum Dot Semiconductor Lasers Operating on the Excited State

Cheng Wang, *Student Member, IEEE*, Benjamin Lingnau, Kathy Lüdge, Jacky Even, and Frédéric Grillot, *Senior Member, IEEE*

***Abstract*— The modulation dynamics and the linewidth enhancement factor of excited-state (ES) lasing quantum dot (QD) semiconductor lasers are investigated through a set of improved rate equation model, in which the contribution of off-resonant states to the refractive index change is taken into account. The ES laser exhibits a broader modulation response associated with a much lower chirp-to-power ratio in comparison with the ground-state (GS) lasing laser. In addition, it is found that the laser emission in ES reduces the linewidth enhancement factor of QD lasers by about 40% than that in GS. These properties make the ES lasing devices, especially InAs/InP ones emitting at 1.55 μm, more attractive for direct modulation in high-speed optical communication systems.**

***Index Terms*— Semiconductor laser, quantum dot, modulation dynamics.**

I. INTRODUCTION

IN MODERN optical communication systems, high-speed semiconductor laser sources are highly requested. Nowadays, owing to the three-dimensional quantum confinement, nanostructure quantum dot (QD) lasers have shown superior properties such as lower transparency current density [1], temperature insensitivity [2] as well as higher tolerance to optical perturbation [3]–[5] compared to their quantum well (QW) and bulk counterparts. As a result, the QD laser becomes an attractive candidate for applications in worldwide telecommunication networks and in future photonics integrated circuits [6]. QD lasers are usually engineered so as to operate on the ground state (GS) optical transition because of its low operation current in contrast to the higher-energy bound states. Nevertheless, several groups pointed out one major drawback of the GS lasing emission concerning the small modulation bandwidth, which is inherently limited by the slow carrier dynamics [7]–[12], the low differential gain as well as the large gain compression factor [13], [14]. On the other hand, chirp-free operation is crucial for directly-modulated laser devices to counteract the chromatic dispersion in standard single mode fibres and thus to enhance the allowable transmission bit rate for a given distance. The frequency chirp property of a semiconductor laser device is known to be directly connected with the linewidth enhancement factor (LEF, also known as alpha factor). QD lasers operating at the GS transition do have the possibility to achieve a near-zero LEF and low frequency chirp [15]–[17], however, the reported LEFs vary over a wide range up to more than 10 [18], [19]. Therefore, it is of great significance to engineer reliable QD laser sources of broad bandwidth, reduced LEF associated with low frequency chirp. Stimulated emission from QD excited state (ES) could be a promising alternative to enhance the laser's dynamic performance.

In practice, the ES emission can be achieved by increasing the bias current, shortening the cavity length, coating the cavity facets or via coupling gratings [20]–[24]. However, ES lasing devices draw less attention because of the high operation current as well as the short wavelength located out of the optical communication windows in the fibre (1.3 μm and 1.55 μm). However, in the InAs/InP QD material system, the GS laser has potential to emit at 1.60 $\sim$ 1.65 μm [25], which is much longer than the communication window. Consequently, since the ES has a higher optical transition energy than the GS, it is possible to tune the ES emission close to 1.55 μm through a proper band energy engineering like the double cap procedure [26]. On the other hand, the ES in QDs shows faster carrier capture rates from the surrounding carrier reservoir states (RS) as well as a higher saturated gain than the GS [20], [21]. Indeed, QD lasers operating on the ES has shown a broader modulation bandwidth and the K-factor limited

Manuscript received April 23, 2014; revised May 27, 2014; accepted June 30, 2014. Date of publication July 8, 2014; date of current version July 25, 2014. The work of C. Wang was supported by the China Scholarship Council. The work of J. Even was supported by Deutscher Akademischer Austauschdienst (DAAD). The work of B. Lingnau and K. Lüdge was supported by the German Research Foundation within the framework SFB 787. The work of F. Grillot was supported in part by the European Office of Aerospace Research and Development under Grant FA8655-12-1-2093 and in part by the Partenariat Huber Curien under Grant 30794RC (Campus France/DAAD).

C. Wang is with the Université Européenne de Bretagne, Rennes Cedex 7 35708, France, and also with Telecom Paristech, Ecole Nationale Supérieure des Télécommunications, Paris 75013, France (e-mail: cheng.wang@insa-rennes.fr).

B. Lingnau and K. Lüdge are with the Insitut für Theoretische Physik, Technische Universität Berlin, Berlin D-10623, Germany (e-mail: lingnau@mailbox.tu-berlin.de; kathy.luedge@tu-berlin.de).

J. Even is with the Université Européenne de Bretagne, Rennes Cedex 7 35708, France (e-mail: jacky.even@insa-rennes.fr).

F. Grillot is with Telecom Paristech, Ecole Nationale Supérieure des Télécommunications, Paris 75013, France (e-mail: frederic.grillot@telecom-paristech.fr).

Color versions of one or more of the figures in this paper are available online at http://ieeexplore.ieee.org.

Digital Object Identifier 10.1109/JQE.2014.2335811

bandwidth is estimated almost twice of that in the GS lasing [20], [21], [27]. A recent work has demonstrated a ES emission InAs/GaAs QD laser with a large-signal modulation capability up to 22.5 Gbps [28]. In addition, the ES emission exhibits a smaller LEF in comparison with the GS emission in a QD laser [29], [30].

In this work, we theoretically investigate the modulation dynamics of the ES lasing in QD lasers employing a coupled rate equation model, in which the carrier capture (from RS to ES) and relaxation (from ES to GS) processes are both considered. Particularly, the model takes into account the contribution of off-resonant states on the refractive index change of the laser, which makes it possible to study the LEF of QD lasers. Through the standard small signal analysis of the QD laser system, it is found that the 3-dB modulation bandwidth of the ES laser is almost 1.5-fold larger than that of the GS one. Meanwhile, calculations show that the ES chirp-to-power ratio (CPR) is reduced by half. The below-threshold LEF of the QD laser is calculated through the amplified spontaneous emission (ASE) technique (also known as Hakki-Paoli method), while the commonly used FM/AM method is employed for extracting the above-threshold LEF. From a semi-classical analysis, it is proved that the GS contributes to the reduction of the LEF in the ES emission QD laser, while the RS increases the LEF value. In addition, the LEF of the ES laser strongly depends on the energy difference between the resonant ES state and the off-resonant states (GS and RS). For the laser under study, the ES lasing LEF is shown to be 40% smaller than that in the GS case.

II. Numerical Model Description

The semiconductor laser system can be microscopically described within the framework of Maxwell's equations and the semiconductor-Bloch equations [31]–[33]. Adiabatically eliminating the microscopic polarizations of the QD and the RS transitions, the optical susceptibility of QD lasers was derived in [34] and [35]. It is assumed that the resonant transitions impact mainly the gain, while having little effect on the refractive index, whereas the off-resonant transitions mainly contribute to the index change. Within the limit of rate equations, the model holds the assumption that the active region consists of only one QD ensemble. The electrons and holes are treated as excitons (neutral pairs) in the model.

In the QD laser, the carriers are firstly injected into the 3-D separate confinement heterostructure (SCH) from the contact, and then diffuse into the 2-D RS [36]. As reported in [7], [11], and [12], the carrier transport process could limit the modulation dynamics. Nevertheless, in order to simplify the rate equation model and analytically analyze the dynamics, this process is not taken into account in this work as already presented in [8] and [18]. Thus as shown in Fig.1, the external injected carriers are assumed to directly fill the RS, from which some of the carriers are captured into the dots. Once in the dots, the carriers relax from the higher energy level ES to the lower level GS. It is noted that a possible direct carrier capture channel from the RS to the GS is not considered in this work [37], which channel can accelerate the carrier scattering

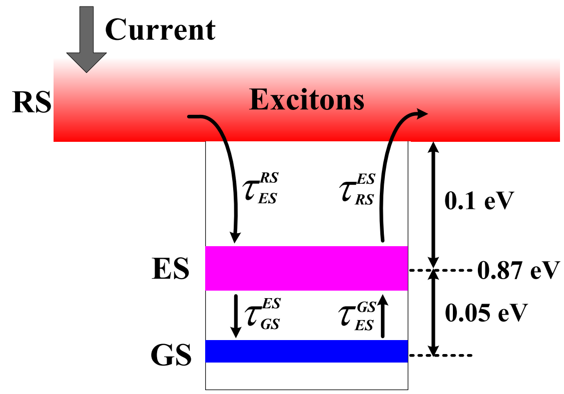

Fig. 1. Schematic of the carrier dynamics in a QD laser. The ES transition energy is 0.87 eV, and its energy separation is 0.1 eV with the RS and 0.05 eV with the GS.

time of the GS. Inversely, carriers can also escape the dots through thermal excitation. In addition, the RS is assumed as a discrete energy state with degeneracy $D_{RS} = k_B T m^* A/(\pi \hbar^2)$, with m^* the reduced exciton mass and A the laser's surface area [18]. Introducing the differential gain a_X (X denotes GS, ES and RS), the gain of each state g_X is given by [38]:

$$g_{GS} = a_{GS} \frac{N_B}{H_B} \left(\frac{2N_{GS}}{2N_B/H_B} - 1 \right) \quad (1)$$

$$g_{ES} = a_{ES} \frac{N_B}{H_B} \left(\frac{2N_{ES}}{4N_B/H_B} - 1 \right) \quad (2)$$

$$g_{RS} = a_{RS} \frac{D_{RS}}{AH_B} \left(\frac{2N_{RS}}{D_{RS}/(AH_B)} - 1 \right) \quad (3)$$

where N_B is the QD surface density, H_B is the height of the dots and N_X denotes the carrier density in each state. The carrier filling in each state induces change of the refractive index, and thus shifts the instantaneous electric field frequency:

$$\Delta\omega_N^{GS} = \frac{1}{2}\Gamma_P v_g g_{GS} F_{GS}^{LS} \quad (4)$$

$$\Delta\omega_N^{ES} = \frac{1}{2}(\Gamma_P v_g g_{ES} - \frac{1}{\tau_P})\alpha_H^{ES} \quad (5)$$

$$\Delta\omega_N^{RS} = \frac{1}{2}\Gamma_P v_g g_{RS} F_{RS}^{LS} \quad (6)$$

with

$$F_{GS,RS}^{LS} = \frac{\omega_{LS}^0}{\omega_{GS,RS}} \frac{(\omega_{GS,RS} - \omega_{LS}^0)T_D}{1 + (\omega_{GS,RS} - \omega_{LS}^0)^2 T_D^2} \quad (7)$$

where $\omega_{GS,RS}$ gives the transition frequency of each state, and ω_{LS}^0 is the lasing frequency in the cold cavity which is resonant with ω_{ES} in the simulations ($\omega_{LS}^0 = \omega_{ES}$). T_D is the polarization dephasing time and τ_P is the photon lifetime, Γ_P is the optical confinement factor and v_g is the group velocity of the light. Due to the dot size dispersion, the inhomogeneous broadening is known to have significant impacts on both static and dynamic characteristics of QD lasers [39]–[41]. This effect can be quantitatively described by a complex multi-population rate equation model [10], [39], which can only be computed numerically. Instead, this work simply introduces an empirical parameter α_H^{ES} in Eq. (5) to describe the resonant ES induced LEF, for which the nonzero value is due to the asymmetric inhomogeneous broadening and the energy renormalization [29], [42]. Then, the slowly varying electric field $E(t)$ is given by

$$\frac{dE(t)}{dt} = \frac{1}{2}\left(\Gamma_P v_g g_{ES} - \frac{1}{\tau_P}\right)E(t) + j\left(\Delta\omega_N^{GS} + \Delta\omega_N^{ES} + \Delta\omega_N^{RS}\right)E(t) \quad (8)$$

The equation holds the assumption that only the resonant ES contributes to the gain. With carrier injection, the lasing frequency becomes $\omega_{LS} = \omega_{th}^{LS} + \Delta\omega_N^{LS}$, where $\Delta\omega_N^{LS} = \Delta\omega_N^{GS} + \Delta\omega_N^{ES} + \Delta\omega_N^{RS}$ gives the frequency shift of the electric field from its threshold value (ω_{th}^{LS}). Via the relationship $E(t) = \sqrt{S(t)V/\Gamma_P}e^{j\phi(t)}$, the photon density $S(t)$ and the phase $\phi(t)$ can be separately described. Combining the carrier dynamics in QD lasers [37], [43], the coupled rate equations for the ES emission laser are finally given by:

$$\frac{dN_{RS}}{dt} = \frac{I}{qV} + \frac{N_{ES}}{\tau_{RS}^{ES}} - \frac{N_{RS}}{\tau_{ES}^{RS}}(1-\rho_{ES}) - \frac{N_{RS}}{\tau_{RS}^{spon}} \quad (9)$$

$$\frac{dN_{ES}}{dt} = \left(\frac{N_{RS}}{\tau_{ES}^{RS}} + \frac{N_{GS}}{\tau_{ES}^{GS}}\right)(1-\rho_{ES}) - \frac{N_{ES}}{\tau_{GS}^{ES}}(1-\rho_{GS}) - \frac{N_{ES}}{\tau_{RS}^{ES}} - \frac{N_{ES}}{\tau_{ES}^{spon}} - v_g g_{ES} S \quad (10)$$

$$\frac{dN_{GS}}{dt} = \frac{N_{ES}}{\tau_{GS}^{ES}}(1-\rho_{GS}) - \frac{N_{GS}}{\tau_{ES}^{GS}}(1-\rho_{ES}) - \frac{N_{GS}}{\tau_{GS}^{spon}} \quad (11)$$

$$\frac{dS}{dt} = \left(\Gamma_P v_g g_{ES} - \frac{1}{\tau_P}\right)S + \beta_{SP}\frac{N_{ES}}{\tau_{ES}^{spon}} \quad (12)$$

$$\frac{d\phi}{dt} = \Delta\omega_N^{GS} + \Delta\omega_N^{ES} + \Delta\omega_N^{RS} \quad (13)$$

where ρ_{GS}, ρ_{ES} are the carrier occupation probabilities in the GS and the ES, respectively. τ_{GS}^{spon} is the spontaneous emission time and β_{SP} is the spontaneous emission factor. Carriers in the RS are scattered into the dots through the phonon-assisted and Auger-assisted processes [44], [45]. The latter makes the scattering rates nonlinearly dependent on the carrier number in the RS, and those can be accurately obtained by a complex microscopic calculation [46], [47]. Nevertheless, in order to simplify the model, the carrier capture time τ_{ES}^{RS} and the relaxation time τ_{GS}^{ES} are both treated as constants. On the other hand, the carrier-escape times (τ_{RS}^{ES}, τ_{ES}^{GS}) are governed by the Fermi distribution for a quasi-thermal equilibrium system [48], [49]. For semiconductor lasers operating under small-signal modulation with frequency ω, the bias current change δI induces variations of carriers δN_X, photon δS and phase $\delta\phi$. Thus, the differential rate equation is derived as follows:

$$\begin{bmatrix} \gamma_{11}+j\omega & -\gamma_{12} & 0 & 0 & 0 \\ -\gamma_{21} & \gamma_{22}+j\omega & -\gamma_{23} & -\gamma_{24} & 0 \\ 0 & -\gamma_{32} & \gamma_{33}+j\omega & 0 & 0 \\ 0 & -\gamma_{42} & 0 & \gamma_{44}+j\omega & 0 \\ -\gamma_{51} & -\gamma_{52} & -\gamma_{53} & 0 & j\omega \end{bmatrix}\begin{bmatrix} \delta N_{RS} \\ \delta N_{ES} \\ \delta N_{GS} \\ \delta S \\ \delta\phi \end{bmatrix} = \frac{\delta I}{qV}\begin{bmatrix} 1 \\ 0 \\ 0 \\ 0 \\ 0 \end{bmatrix} \quad (14)$$

with

$$\begin{aligned}
\gamma_{11} &= \frac{1-\rho_{ES}}{\tau_{ES}^{RS}} + \frac{1}{\tau_{RS}^{spon}};\ \gamma_{12} = \frac{1}{\tau_{RS}^{ES}} + \frac{1}{4N_B}\frac{N_{RS}}{\tau_{ES}^{RS}}; \\
\gamma_{21} &= \frac{1-\rho_{ES}}{\tau_{ES}^{RS}};\ \gamma_{22} = \frac{1-\rho_{GS}}{\tau_{GS}^{ES}} + \frac{1}{\tau_{RS}^{ES}} + \frac{1}{\tau_{ES}^{spon}} \\
&\quad + \frac{1}{4N_B}\frac{N_{RS}}{\tau_{ES}^{RS}} + \frac{1}{4N_B}\frac{N_{GS}}{\tau_{ES}^{GS}} + \frac{1}{2}v_g a_{ES} S; \\
\gamma_{23} &= \frac{1-\rho_{ES}}{\tau_{ES}^{GS}} + \frac{1}{2N_B}\frac{N_{ES}}{\tau_{GS}^{ES}};\ \gamma_{24} = -v_g g_{ES}; \\
\gamma_{32} &= \frac{1-\rho_{GS}}{\tau_{GS}^{ES}} + \frac{1}{4N_B}\frac{N_{GS}}{\tau_{ES}^{GS}}; \\
\gamma_{33} &= \frac{1-\rho_{ES}}{\tau_{ES}^{GS}} + \frac{1}{2N_B}\frac{N_{ES}}{\tau_{GS}^{ES}} + \frac{1}{\tau_{GS}^{spon}}; \\
\gamma_{42} &= \frac{1}{2}\Gamma_P v_g a_{ES} S + \frac{\beta_{SP}}{\tau_{ES}^{spon}};\ \gamma_{44} = -\Gamma_P v_g g_{ES} + \frac{1}{\tau_p}; \\
\gamma_{51} &= \Gamma_P v_g a_{RS} F_{RS}^{ES};\ \gamma_{52} = \frac{1}{4}\Gamma_P v_g a_{ES}\alpha_H^{ES}; \\
\gamma_{53} &= \frac{1}{2}\Gamma_P v_g a_{GS} F_{GS}^{ES};
\end{aligned} \quad (15)$$

The QD laser dynamics can be explored from the above equations as follows:

a) The intensity modulation (IM) response is calculated by [50]:

$$H(j\omega) = \delta S(j\omega)/(\delta I/qV) \quad (16)$$

b) The LEF is of great importance for semiconductor lasers because it influences various fundamental features such as spectral linewidth, mode stability, frequency chirp under modulation, as well as nonlinear dynamics subject to optical injection and optical feedback [51], [52]. The LEF describes the coupling between the carrier-induced refractive index (field frequency) change and the gain change. For conventional bulk and QW lasers, the index part and the gain part are synchronized [51], whereas those are desynchronized for QD lasers [34]. The phase-amplitude coupling $A_{QD}^{ES}(j\omega)$ of the electric field for the ES emission QD laser is

$$A_{QD}^{ES}(j\omega) = \frac{2}{\Gamma_P v_g}\frac{\delta\omega_{LS}}{\delta g_{ES}} \equiv \alpha_H^{ES} + 2F_{GS}^{ES}\frac{a_{GS}}{a_{ES}}\frac{\delta N_{GS}}{\delta N_{ES}} + 4F_{RS}^{ES}\frac{a_{RS}}{a_{ES}}\frac{\delta N_{RS}}{\delta N_{ES}} \quad (17)$$

In the following section, it will be shown that the function $A_{QD}^{ES}(j\omega)$ is actually dependent on the modulation frequency, and its minimum value gives the conventional LEF $\alpha_{H,QD}^{ES}$ of QD lasers, that is,

$$\alpha_{H,QD}^{ES} = \left[A_{QD}^{ES}(j\omega)\right]_{\min} \quad (18)$$

Experimentally, various techniques have been proposed for the measurement of the LEF [51], [53]. In this work, we employ the widely used FM/AM technique for extracting the above-threshold LEF, while the ASE method is used for obtaining the below-threshold one. The FM/AM technique relies on the direct current modulation of the laser, which generates both optical frequency (FM) and amplitude (AM) modulations [54]. Then, the LEF is extracted by taking the minimum ratio of the FM index ($\beta(j\omega)$) to the AM index ($m(j\omega)$) as $\alpha_{H,QD}^{FM/AM} = [2\beta(j\omega)/m(j\omega)]_{\min}$. Correspondingly, from Eqs. (14) and (15) we obtain

$$\begin{aligned}\alpha_{H,QD}^{FM/AM} &= \left[2\frac{\delta\omega_{LS}/\omega}{\delta S/S}\right]_{\min} \\ &\equiv \Bigg[\frac{j\omega + 1/\tau_p - \Gamma_p v_g g_{ES}}{j\omega} \\ &\times\left(\alpha_H^{ES} + 2F_{GS}^{ES}\frac{a_{GS}}{a_{ES}}\frac{\delta N_{GS}}{\delta N_{ES}} + 4F_{RS}^{ES}\frac{a_{RS}}{a_{ES}}\frac{\delta N_{RS}}{\delta N_{ES}}\right)\Bigg]_{\min}\end{aligned} \tag{19}$$

For semiconductor lasers operating below threshold, slightly tuning the pump current (ΔI) without any modulation will change the carrier density as ΔN_X. The LEF can be extracted from the direct measurement of the gain and wavelength (refractive index, field frequency) changes by monitoring the variation of longitudinal modes in the laser cavity [13]. Thus, the below-threshold LEF is calculated by

$$\begin{aligned}\alpha_{H,QD}^{ASE} = \frac{2}{\Gamma_P v_g}\frac{\Delta\omega_{LS}}{\Delta g_{ES}} &\equiv \alpha_H^{ES} + 2F_{GS}^{ES}\frac{a_{GS}}{a_{ES}}\frac{\Delta N_{GS}}{\Delta N_{ES}} \\ &+ 4F_{RS}^{ES}\frac{a_{RS}}{a_{ES}}\frac{\Delta N_{RS}}{\Delta N_{ES}}\end{aligned} \tag{20}$$

It is noted that for the sake of simplicity, the gain compression contribution is not indicated in expressions (17)–(20). Nevertheless, the gain compression effect has been taken into account in the numerical results of the LEF presented hereafter.

c) Generally, QD lasers have high gain compression factors (ξ) in the range of $10^{-16} \sim 10^{-15}$ cm^3, which are one or two orders of magnitude larger than those in QW lasers [14], [55]. The gain compression effect is modeled by improving the gain expression as

$$g_{ES} \rightarrow \frac{g_{ES}}{1 + \xi S} \tag{21}$$

Using the improved gain expression, the frequency chirp property of the QD laser is characterized by the CPR as [56]:

$$CPR_{ES}(j\omega) = \frac{\delta\omega_{LS}(\omega)}{\delta S(\omega)} \approx \frac{\alpha_{H,QD}^{ES}}{2S}\left(j\omega + \Gamma_p v_g a_{ES}^p S\right) \tag{22}$$

with $a_{ES}^p = -\partial g_{ES}/\partial S$. The above threshold relation $\Gamma_p v_g g_{ES} \approx 1/\tau_p$ has been used in the above equation.

In order to compare the dynamic performance with a laser operating on the GS, rate equations (9)-(13) can be rewritten by considering the stimulated emission in Eq. (11) instead of Eq. (10), and the electric field is modified correspondingly. Following a similar approach of small-signal analysis as above, the analytical expressions for the GS lasing dynamics can be derived [38]. It is noted that simultaneous lasing on the GS and ES is not considered in this work [37].

TABLE I

MATERIAL PARAMETERS AND LASER PARAMETERS

Symbol	Parameter	Value
E_{RS}	RS transition energy	0.97 eV
E_{ES}	ES transition energy	0.87 eV
E_{GS}	GS transition energy	0.82 eV
τ_{ES}^{RS}	Capture time from RS to ES	12.6 ps
τ_{GS}^{ES}	Relaxation time from ES to GS	5.8 ps
τ_{RS}^{spon}	Spontaneous decay time of RS	500 ps
τ_{ES}^{spon}	Spontaneous decay time of ES	500 ps
τ_{GS}^{spon}	Spontaneous decay time of GS	1200 ps
Γ_p	Optical confinement factor	0.06
β_{SP}	Spontaneous emission factor	1×10^{-4}
ξ	Gain compression factor	2×10^{-16} cm^3
L	Active region length	5×10^{-2} cm
W	Active region width	4×10^{-4} cm
$R_1=R_2$	Mirror reflectivity	0.32
n_r	Refractive index	3.5
α_i	Internal modal loss	6 cm^{-1}
N	Number of QD layers	5
N_B	Dot density	10×10^{10} cm^{-2}
H_B	Dot height	5×10^{-7} cm
a_{GS}	GS differential gain	5×10^{-15} cm^2
a_{ES}	ES differential gain	10×10^{-15} cm^2
a_{RS}	RS differential gain	2.5×10^{-15} cm^2
α_H^{GS}	GS induced LEF	0.5
α_H^{ES}	ES induced LEF	0.5
T_D	Dephasing time	0.1 ps

III. COMPARISON OF THE DYNAMICAL PROPERTIES FOR QD LASING ON THE GS AND ON THE ES

The laser under study is based on the InAs/InP(311B) QD structure [11], and the laser device parameters used in the simulation are listed in Table 1 [57]–[59]. One can select the sole lasing on the ES (GS) by facet coating in order to suppress the GS (ES) lasing. The facet reflectivity for the lasing mode is set as $R_1 = 0.32$. The internal loss parameter ($\alpha_i = 6$ cm^{-1}) is assumed to be constant [39] and to be independent of the free carrier density in the waveguide [60]. The cavity length as well as other parameters in the table is kept the same for comparison. In such way, Figure 2 compares the steady-state solutions of lasing in the ES (Fig. 2(a)) and in the GS (Fig. 2(b)). The threshold current of ES lasing is about 90 mA, which is 1.8-fold larger than that of the GS. In Fig. 2(a), carriers both in ES and GS are clamped above threshold, and the former population is larger due to the higher degeneracy of ES than GS. Thus, despite a higher threshold current the ES does provide a larger saturated gain. In figure 2(b), however, the carrier population in the ES keeps increasing when the GS laser reaches the threshold current.

Through Eq. (16), the calculated IM responses for GS and ES lasing operations are shown in Fig. 3(a), respectively. As observed, the ES response indeed exhibits a broader and flatter response in contrast to the GS one. The broader bandwidth is attributed partly to the faster carrier capture time [20], as well as to the higher ES differential gain (a_{ES}) [21], which

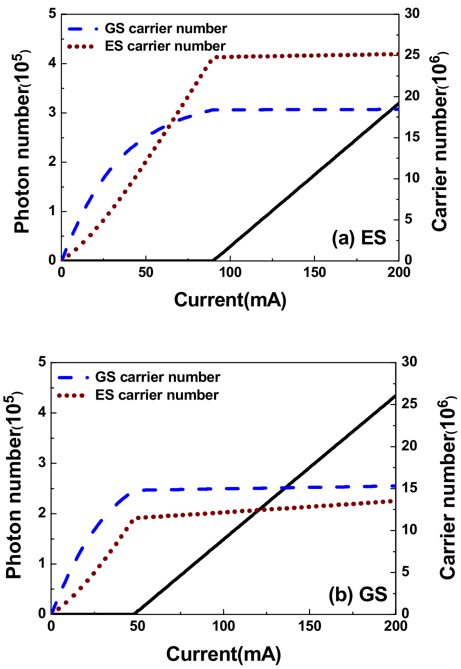

Fig. 2. Steady-state solution for (a) lasing in the ES and (b) lasing in the GS. Solid lines denote the photon number, dashed and dotted lines represent the carrier number in the GS and ES, respectively.

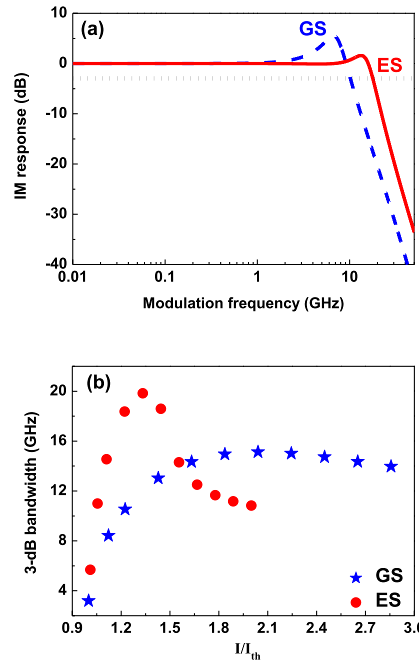

Fig. 3. (a) Intensity modulation response versus modulation frequency. The dotted line indicates the 3-dB modulation bandwidth. (b) 3-dB bandwidth for stimulated emissions in the ES and GS, respectively. The bias currents are set at $I_{ES} = 1.2 \times I_{th,ES}$ and $I_{GS} = 1.2 \times I_{th,GS}$.

is set two-folder larger than the GS one (a_{GS}) as listed in Table I. However, it is noted that the values of the differential gain in QD lasers can vary in a wide range in the order of $10^{-16} \sim 10^{-14}$ cm^2 [13], [61]. The lower resonance peak in the ES response indicates a stronger damping factor. From the IM response curve, the 3-dB modulation bandwidth is extracted and depicted in Fig. 3(b) as a function of the normalized bias current (I/I_{th}). The ES and GS bandwidths firstly increase with the bias current and then reach a maximum value. The calculated maximum ES bandwidth is about 5 GHz larger than the GS case. Further increase of the bias current reduces the bandwidth because the modulation response becomes over-damped [11], [12]. It is found that the ES bandwidth decreases faster than the GS lasing case, which means that the ES damping factor is more sensitive to the bias current. It is noted that the carrier transport process from the SCH as well as the inhomogeneous broadening in the QDs can further reduce the 3-dB bandwidth described in Fig. 3 [41].

With respect to Eq. (22), Fig. 4(a) presents the CPR response of the ES laser. In the so-called adiabatic chirp regime, the gain compression dominates and the CPR can be approximated by $\Gamma_p v_g a^p_{ES} \alpha^{ES}_{H,QD}/2$. As the thermal effect is not included, the CPR remains constant at a low level less than 1 GHz/mW for modulation frequencies below 1 GHz. For higher modulation frequencies, the CPR rises almost parabolically with the modulation frequency following the relation $j\omega\alpha^{ES}_{H,QD}/(2S)$. Due to the reduced LEF in the ES (this will be discussed in the following section), the ES lasing CPR is found always smaller than the GS case. The discrepancy becomes larger at high modulation frequencies. For instance, at 20 GHz the CPR of the ES laser is 60%

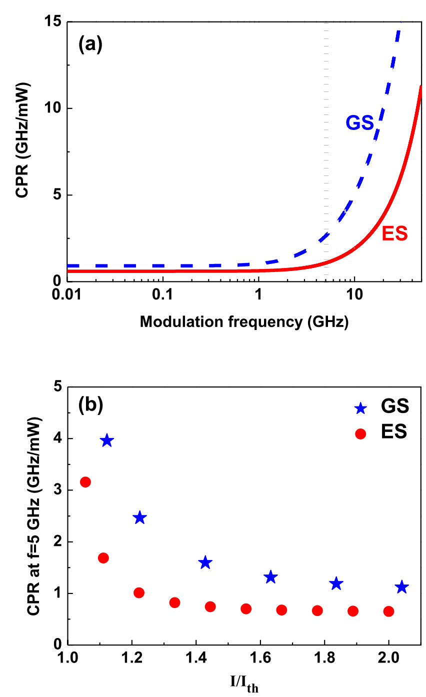

Fig. 4. (a) CPR response versus the modulation frequency with respect to Eq. (22). The bias currents are set at $I_{ES} = 1.2 \times I_{th,ES}$ and $I_{GS} = 1.2 \times I_{th,GS}$, respectively. The dotted line indicates CPR at modulation frequency f = 5.0 GHz (b) CPR variation as a function of the normalized bias current (I/I_{th}) at f = 5.0 GHz.

smaller than that in the GS configuration. Figure 4(b) shows the CPR calculated at a fixed modulation frequency (5 GHz) as a function of the bias current. The CPR decreases with the pump current because of the higher output power and finally

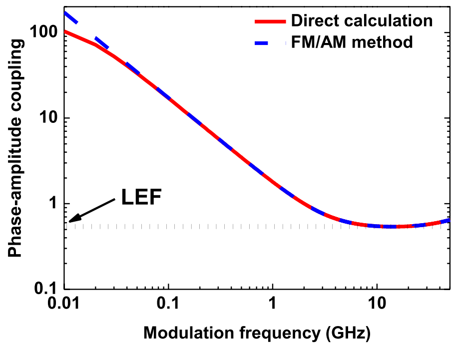

Fig. 5. Frequency dependence of the phase-amplitude coupling of the electric field for the ES lasing at $I = 1.2 \times I_{th}$. The direct calculation follows Eq. (17), and the FM/AM method follows Eq. (19). Note that the gain compression effect is included in the plot. The minimum level of the curve gives the LEF value (dotted line).

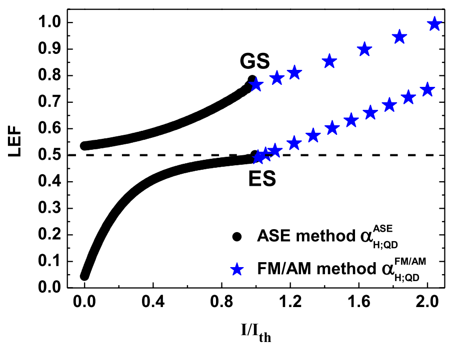

Fig. 6. A comparison on the LEFs between the ES and GS emission lasers. The dashed line gives the resonant state contributed part (0.5) of LEF.

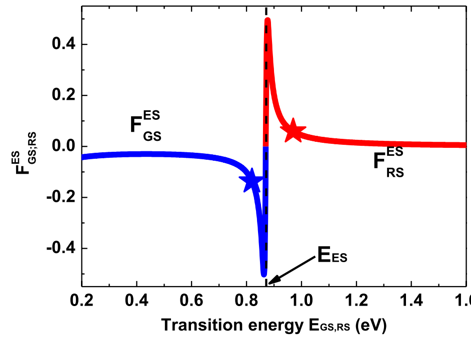

Fig. 7. Dependence of the $F_{GS,RS}^{ES}$ parameters on the GS-ES and ES-RS energy separations in the case of a QD laser emitting on its excited state. The dashed line indicates the ES emission energy of $E_{ES} = 0.87$ eV, and the stars denote $F_{GS,RS}^{ES}$ values used in this work.

reaches a finite value. Still, the ES CPR remains lower than the GS CPR level. Since directly-modulated semiconductor lasers suffer significantly from the frequency chirp, these results make the ES lasing transmitters very promising for the optical communication networks.

Figure 5 presents the phase-amplitude coupling of the electric field as a function of modulation frequency. It shows that the modulation index ratio $2\beta(j\omega)/m(j\omega)$ (dashed curve) obtained from Eq. (19) is highly consistent with the direct calculation $A_{QD}^{ES}(j\omega)$ (solid curve) extracted from Eq. (17). Only a slight discrepancy arises at very low frequencies due to the gain compression. The plots prove that the phase-amplitude coupling ratio is strongly dependent on the modulation frequency [62]. The coupling magnitude is rather high at low modulation frequency and decreases to a plateau when increasing the frequency. Conventionally, the LEF of semiconductor lasers is given by this minimum as indicated by the dotted line. As we can see, the LEF obtained from Eq. (19) matches quite well with the one calculated from Eq. (18), i.e., $\alpha_{H,QD}^{ES} \approx \alpha_{H,QD}^{FM/AM}$. In contrast to QW lasers, further increase of the modulation frequency could raise the coupling ratio as already reported in [52] and [63].

Figure 6 compares the variations of ES and GS LEFs with the injected current. Below threshold, carriers in both resonant and off-resonant states increase with the pump current and the LEFs rise nonlinearly. Above threshold, the carrier population in the resonant state is clamped while the LEF evolution becomes relatively linear. At threshold, it is found that the LEFs extracted from the ASE method and from the FM/AM method are in good agreement. For both below and above threshold, the predicted ES LEF is found always smaller than the GS one. The ES lasing LEF at threshold is reduced by about 40% in contrast to the GS lasing case. It is noted that the GS LEF is always larger than the resonant GS state contributed part ($\alpha_H^{GS} = 0.5$), whereas the ES LEF can be smaller than that ($\alpha_H^{ES} = 0.5$). In order to explore the underlying mechanisms, we write the LEF expression for lasing in the GS [38]:

$$\alpha_{H,QD}^{GS} = \left[\alpha_H^{GS} + \frac{1}{2}F_{ES}^{GS}\frac{a_{ES}}{a_{GS}}\frac{\delta N_{ES}}{\delta N_{GS}} + 2F_{RS}^{GS}\frac{a_{RS}}{a_{GS}}\frac{\delta N_{RS}}{\delta N_{GS}}\right]_{\min} \tag{23}$$

with

$$F_{ES,RS}^{GS} = \frac{\omega_{GS}}{\omega_{ES,RS}}\frac{(\omega_{ES,RS}-\omega_{GS})T_D}{1+(\omega_{ES,RS}-\omega_{GS})^2T_D^2} \tag{24}$$

Because the off-resonant state energies of ES ($\hbar\omega_{ES}$) and RS ($\hbar\omega_{RS}$) are both higher than the GS one ($\hbar\omega_{GS}$) we obtain $F_{ES}^{GS} > 0$ and $F_{RS}^{GS} > 0$ in Eq. (24). So in the case of the QD laser operating on the GS transition, both the ES and the RS contribute to enhance the LEF [64], [65]. In contrast for the ES lasing case depicted in Eq. (7) where $F_{GS}^{ES} < 0$ and $F_{RS}^{ES} > 0$, the lower-energy GS contributes to reduce the LEF of ES laser while the RS remains increase its value. Therefore when the GS contributes more than the RS, the ES lasing LEF will become smaller than the resonant ES state induced part.

IV. Effect of QD Electronic Structure on the ES LEF

Equations (7) and (24) also indicate that the LEF value strongly depends on the energy separation between the resonant state and the off-resonant states. Figure 7 presents the variations of the $F_{GS,RS}^{ES}$ parameters for the ES emission as a function of GS-ES and ES-RS energy separations. For small energy separation values (~0.01 eV) the parameters $F_{GS,RS}^{ES}$ undergo drastic variations, followed by a rapid increase (decrease) with the enlarged energy split. It is also shown that those off-resonant states have little contribution to the LEF when the energy separation becomes larger than 0.25 eV.

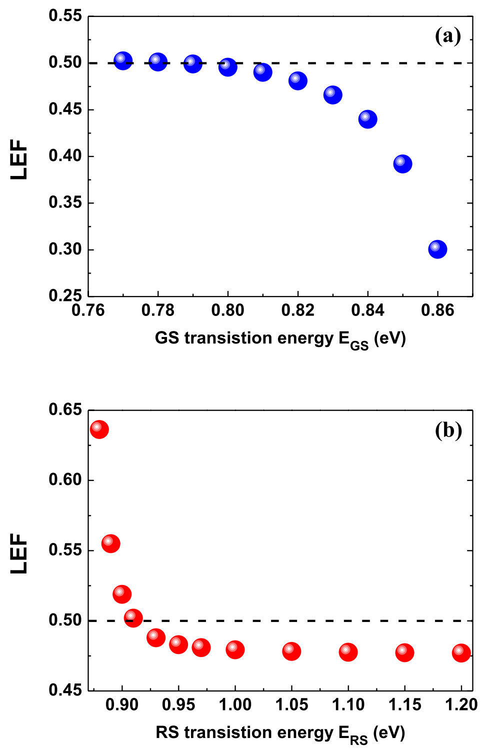

Fig. 8. LEF dependence on the off-resonant state transition energy for the ES emission laser with $E_{ES} = 0.87$ eV (a) as a function of GS transition energy E_{GS}, with $E_{RS} = 0.97$ eV; (b) as a function of RS transition energy E_{RS}, with $E_{GS} = 0.82$ eV. The dashed line indicates the resonant ES contributed part of the LEF. The bias current is fixed at $I=0.9 \times I_{th,ES}$.

Figure 8 depicts the below threshold LEF dependence on the transition energy ($I = 0.9 \times I_{th,ES}$). Indeed, when the GS is localized far away from the ES, the GS has little influence on the LEF value (Fig. 8(a)). But once the band gap is less than 60 meV, the LEF decreases rapidly with increasing GS transition energy E_{GS}. For a band gap of 10 meV, the LEF value is reduced by about 40%. In contrast, Fig. 8(b) illustrates that small energy separation between the RS and the ES leads to a large α-factor. When the separation is less than 40 meV, the laser exhibits a higher value than the ES induced part, which means the RS contributes more than the GS on the α-factor. Increasing the RS energy E_{RS} reduces the LEF and finally leads to a limit value of about 0.48 when the ES-RS separation is larger than 80 meV. Therefore, in order to reduce the LEF of the ES emission laser, one potential option is to diminish the energy separation with the GS or (and) to enlarge the separation with the RS. In InAs/InP or InAs/GaAs material systems, the GS transition energy is mostly determined by the vertical confinement and thus the thickness of the QD, while the energy splits are related to QD lateral confinement [66]–[68]. In consequence, the simulation results provide some basic guidance for the fabrication of zero or even negative LEFs of QD lasers through proper quantum engineering of the bound and continuum states.

V. Conclusion and Future Work

The ES lasing dynamics of a QD laser are studied through an improved rate equation model in comparison with the GS lasing one. It is found that although the ES laser requires a higher operation current, it provides a larger modulation bandwidth and a lower frequency chirp, which are much superior to those of GS lasers. In addition, the ES laser exhibits a smaller LEF due to the contribution of the lower energy off-resonant GS state. From the semi-analytical analysis, calculations prove the possibility of reducing the ES lasing LEF to zero or even negative values through the band energy engineering. This work paves the way for the realization of high speed, chirp free directly-modulated semiconductor laser sources for applications in the future optical telecommunication networks. Future work will take into account the inhomogeneous broadening through a multi-population rate equation model as well as the carrier transport process from the 3-D SCH to the 2-D RS. In addition, the chosen parameters listed in Table 1 do not necessarily lead to an optimal ES lasing operation. We believe that, the present theoretical model will put forward QD lasers operating on the ES state. For that purpose, it will be essential to optimize the optical loss (photon lifetime) by properly controlling the cavity length or the facet reflectivity so as to further enhance the dynamic performance [60], [69].

Acknowledgment

The authors would like to thank Professors Ivo Montrosset, Mariangela Gioannini from Politecnico di Torino, Italy and Eckehard Schöll from Technische Universität Berlin, Germany for fruitful discussions.

References

[1] G. T. Liu, A. Stintz, H. Li, K. J. Malloy, and L. F. Lester, "Extremely low room-temperature threshold current density diode lasers using InAs dots in $In_{0.15}Ga_{0.85}As$ quantum well," *Electron. Lett.*, vol. 35, no. 14, pp. 1163–1165, 1999.

[2] S. S. Mikhrin *et al.*, "High power temperature-insensitive 1.3 µm InAs/InGaAs/GaAs quantum dot lasers," *Semicond. Sci. Technol.*, vol. 20, no. 5, pp. 340–342, 2005.

[3] G. Huyet *et al.*, "Quantum dot semiconductor lasers with optical feedback," *Phys. Status Solidi (A)*, vol. 201, no. 2, pp. 345–352, 2004.

[4] K. Lüdge and H. G. Schuster, *Nonlinear Laser Dynamics: From Quantum Dots to Cryptography*. New York, NY, USA: Wiley, 2012.

[5] C. Otto, *Dynamics of Quantum Dot Lasers: Effects of Optical Feedback and External Optical Injection*. Berlin, Germany: Springer-Verlag, 2014.

[6] M. T. Crowley, N. A. Naderi, H. Su, F. Grillot, and L. F. Lester, "GaAs based quantum dot lasers," in *Advances in Semiconductor Lasers, Semiconductors and Semimetals*, vol. 86, J. J. Coleman and A. C. Bryce, Eds. New York, NY, USA: Academic, 2012, pp. 371–417.

[7] F. Lelarge *et al.*, "Recent advances on InAs/InP quantum dash based semiconductor lasers and optical amplifiers operating at 1.55 μm," *IEEE J. Sel. Topics Quantum Electron.*, vol. 13, no. 1, pp. 111–124, Jan./Feb. 2007.

[8] C. Wang, F. Grillot, and J. Even, "Impacts of wetting layer and excited state on the modulation response of quantum-dot lasers," *IEEE J. Quantum Electron.*, vol. 48, no. 9, pp. 1144–1150, Sep. 2012.

[9] B. Lingnau, K. Lüdge, W. W. Chow, and E. Schöll, "Influencing modulation properties of quantum-dot semiconductor lasers by carrier lifetime engineering," *Appl. Phys. Lett.*, vol. 101, no. 13, pp. 131107-1–131107-4, 2012.

[10] M. Gioannini and M. Rossetti, "Time-domain traveling wave model of quantum dot DFB lasers," *IEEE J. Sel. Topics Quantum Electron.*, vol. 17, no. 5, pp. 1318–1326, Sep./Oct. 2011.

[11] L. V. Asryan, Y. Wu, and R. A. Suris, "Carrier capture delay and modulation bandwidth in an edge-emitting quantum dot laser," *Appl. Phys. Lett.*, vol. 98, no. 13, pp. 131108-1–131108-3, 2011.

[12] Y. Wu, R. A. Suris, and L. V. Asryan, "Effect of excited states on the ground-state modulation bandwidth in quantum dot lasers," *Appl. Phys. Lett.*, vol. 102, no. 19, pp. 191102-1–191102-5, 2013.

[13] A. Martinez *et al.*, “Dynamic properties of InAs/InP (311)B quantum dot Fabry–Perot lasers emitting at 1.52 μm,” *Appl. Phys. Lett.*, vol. 93, no. 2, pp. 021101-1–021101-3, Jul. 2008.

[14] A. E. Zhukov *et al.*, “Gain compression and its dependence on output power in quantum dot lasers,” *J. Appl. Phys.*, vol. 113, no. 23, pp. 233103-1–233103-5, Jun. 2013.

[15] T. C. Newell, D. J. Bossert, A. Stintz, B. Fuchs, K. J. Malloy, and L. F. Lester, “Gain and linewidth enhancement factor in InAs quantum-dot laser diodes,” *IEEE Photon. Technol. Lett.*, vol. 11, no. 12, pp. 1527–1529, Dec. 1999.

[16] Z. Mi, P. Bhattacharya, and S. Fathpour, “High-speed 1.3 μm tunnel injection quantum-dot lasers,” *Appl. Phys. Lett.*, vol. 86, no. 15, pp. 153109-1–153109-3, 2005.

[17] H. Saito, K. Nishi, A. Kamei, and S. Sigou, “Low chirp observed in directly modulated quantum dot lasers,” *IEEE Photon. Technol. Lett.*, vol. 12, no. 10, pp. 1298–1230, Oct. 2000.

[18] A. Markus, J. X. Chen, O. Gauthier-Lafaye, J. Provost, C. Paranthoen, and A. Foire, “Impact of intraband relaxation on the performance of a quantum-dot laser,” *IEEE J. Sel. Topics Quantum Electron.*, vol. 9, no. 5, pp. 1308–1314, Sep./Oct. 2003.

[19] B. Dagens *et al.*, “Giant linewidth enhancement factor and purely frequency modulated emission from quantum dot laser,” *Electron. Lett.*, vol. 41, no. 6, pp. 323–324, Mar. 2005.

[20] B. J. Stevens, D. T. D. Childs, H. Shahid, and R. A. Hogg, “Direct modulation of excited state quantum dot lasers,” *Appl. Phys. Lett.*, vol. 95, no. 6, pp. 061101-1–061101-3, Aug. 2009.

[21] C.-S. Lee, P. Bhattacharya, T. Frost, and W. Guo, “Characteristics of a high speed 1.22 μm tunnel injection p-doped quantum dot excited state laser,” *Appl. Phys. Lett.*, vol. 98, no. 1, pp. 011103-1–011103-3, 2011.

[22] X. Q. Lv, P. Jin, W. Y. Wang, and Z. G. Wang, “Broadband external cavity tunable quantum dot lasers with low injection current density,” *Opt. Exp.*, vol. 18, no. 9, pp. 8916–8922, 2010.

[23] G. Lin, P.-Y. Su, and H.-C. Cheng, “Low threshold current and widely tunable external cavity lasers with chirped multilayer InAs/InGaAs/GaAs quantum-dot structure,” *Opt. Exp.*, vol. 20, no. 4, pp. 3941–3947, 2012.

[24] C. Paranthoen, “Growth and optical characterizations of InAs quantum dots on InP substrate: Towards a 1.55 μm quantum dot laser,” *J. Cryst. Growth.*, vol. 251, nos. 1–4, pp. 230–235, 2003.

[25] C. Wang *et al.*, “Nondegenerate four-wave mixing in a dual-mode injection-locked InAs/InP(100) nanostructure laser,” *IEEE Photon. J.*, vol. 6, no. 1, p. 1500408, Feb. 2014.

[26] C. Cornet *et al.*, “Electronic and optical properties of InAs/InP quantum dots on InP(100) and InP(311)B substrates: Theory and experiment,” *Phys. Rev. B*, vol. 74, no. 3, pp. 035312-1–156312-9, 2006.

[27] P.-F. Xu *et al.*, “Temperature-dependent modulation characteristics for 1.3 μm InAs/GaAs quantum dot lasers,” *J. Appl. Phys.*, vol. 107, no. 1, pp. 013102-1–013102-5, Jan. 2010.

[28] D. Arsenijevi *et al.*, “Comparison of dynamic properties of ground- and excited-state emission in p-doped InAs/GaAs quantum-dot lasers,” *Appl. Phys. Lett.*, vol. 104, no. 18, pp. 181101-1–181101-5, May 2014.

[29] P.-F. Xu, H.-M. Ji, J.-L. Xiao, Y.-Z. Huang, and T. Yang, “Reduced linewidth enhancement factor due to excited state transition of quantum dot lasers,” *Opt. Lett.*, vol. 37, no. 8, pp. 1298–1300, 2012.

[30] J.-L. Xiao *et al.*, “Measurement of linewidth enhancement factor for 1.3-μm InAs/GaAs quantum dot lasers,” *IEEE Photon. Technol. Lett.*, vol. 25, no. 5, pp. 488–491, Mar. 1, 2013.

[31] W. W. Chow and S. W. Koch, “Theory of semiconductor quantum-dot laser dynamics,” *IEEE J. Quantum Electron.*, vol. 41, no. 4, pp. 495–505, Apr. 2005.

[32] W. W. Chow and F. Jahnke, “On the physics of semiconductor quantum dots for applications in lasers and quantum optics,” *Prog. Quantum Electron.*, vol. 37, no. 3, pp. 109–184, 2013.

[33] B. Lingnau, K. Lüdge, E. Schöll, and W. W. Chow, “Many-body and nonequilibrium effects on relaxation oscillations in a quantum-dot microcavity laser,” *Appl. Phys. Lett.*, vol. 97, no. 11, pp. 111102-1–111102-3, Sep. 2010.

[34] B. Lingnau, K. Lüdge, W. W. Chow, and E. Schöll, “Failure of the α factor in describing dynamical instabilities and chaos in quantum-dot lasers,” *Phys. Rev. E*, vol. 86, no. 6, pp. 065201-1–065201-5(R) 2012.

[35] B. Lingnau, W. W. Chow, E. Schöll, and K. Lüdge, “Feedback and injection locking instabilities in quantum-dot lasers: A microscopically based bifurcation analysis,” *New J. Phys.*, vol. 15, no. 9, pp. 093031-1–093031-25, 2013.

[36] M. Rossetti, P. Bardella, and I. Montrosset, “Time-domain travelling-wave model for quantum dot passively mode-locked lasers,” *IEEE J. Quantum Electron.*, vol. 47, no. 2, pp. 139–150, Feb. 2011.

[37] K. Veselinov *et al.*, “Analysis of the double laser emission occurring in 1.55-μm InAs–InP (113)B quantum-dot lasers,” *IEEE J. Quantum Electron.*, vol. 43, no. 9, pp. 810–816, Sep. 2007.

[38] C. Wang, J. Even, and F. Grillot, “Near-threshold relaxation dynamics of a quantum dot laser,” *Proc. SPIE, Semicond. Lasers Laser Dyn. VI*, vol. 9134, p. 913404, May 2014.

[39] M. Sugawara, K. Mukai, Y. Nakata, H. Ishikawa, and A. Sakamoto, “Effect of homogeneous broadening of optical gain on lasing spectra in self-assembled $In_XGa_{1-X}As/GaAs$ quantum dot lasers,” *Phys. Rev. B*, vol. 61, no. 11, pp. 7595–7603, Mar. 2000.

[40] L. V. Asryan and R. A. Suris, “Upper limit for the modulation bandwidth of a quantum dot laser,” *Appl. Phys. Lett.*, vol. 96, no. 22, pp. 221112-1–221112-3, May 2010.

[41] L. V. Asryan and R. A. Suris, “Inhomogeneous line broadening and the threshold current density of a semiconductor quantum dot laser,” *Semicond. Sci. Technol.*, vol. 11, no. 4, pp. 554–567, 1996.

[42] H. C. Schneider, W. W. Chow, and S. W. Koch, “Many-body effects in the gain spectra of highly excited quantum-dot lasers,” *Phys. Rev. B*, vol. 64, no. 11, pp. 115315-1–115315-7, 2001.

[43] F. Grillot, C. Wang, N. A. Naderi, and J. Even, “Modulation properties of self-injected quantum-dot semiconductor diode lasers,” *IEEE J. Sel. Topics Quantum Electron.*, vol. 19, no. 4, p. 1900812, Jul./Aug. 2013.

[44] B. Ohnesorge, M. Albrecht, J. Oshinowo, A. Forchel, and Y. Arakawa, “Rapid carrier relaxation in self-assembled $In_XGa_{1-X}As/GaAs$ quantum dots,” *Phys. Rev. B*, vol. 54, no. 16, pp. 11532–11538, 1996.

[45] I. V. Ignatiev, I. E. Kozin, S. V. Nair, H. W. Ren, S. Sugou, and Y. Masumoto, “Carrier relaxation dynamics in InP quantum dots studied by artificial control of nonradiative losses,” *Phys. Rev. B*, vol. 61, no. 23, pp. 15633–15636, 2000.

[46] N. Majer, K. Lüdge, and E. Schöll, “Cascading enables ultrafast gain recovery dynamics of quantum dot semiconductor optical amplifiers,” *Phys. Rev. B*, vol. 82, no. 23, pp. 235301-1–235301-6, 2010.

[47] J. Pausch, C. Otto, E. Tylaite, N. Majer, E. Schöll, and K. Lüdge, “Optically injected quantum dot lasers: Impact of nonlinear carrier lifetimes on frequency-locking dynamics,” *New J. Phys.*, vol. 14, no. 5, p. 053018, 2012.

[48] K. Lüdge and E. Schöll, “Quantum-dot lasers—Desynchronized nonlinear dynamics of electrons and holes,” *IEEE J. Quantum Electron.*, vol. 45, no. 11, pp. 1396–1403, Nov. 2009.

[49] F. Grillot *et al.*, “Spectral analysis of 1.55-μm InAs–InP(113)B quantum-dot lasers based on a multipopulation rate equations model,” *IEEE J. Quantum Electron.*, vol. 45, no. 7, pp. 872–878, Jul. 2009.

[50] L. A. Coldren and S. W. Corzine, *Diode Lasers and Photonic Integrated Circuits*. New York, NY, USA: Wiley, 1995.

[51] M. Osinski and J. Buus, “Linewidth broadening factor in semiconductor lasers—An overview,” *IEEE J. Quantum Electron.*, vol. QE-23, no. 1, pp. 9–29, Jan. 1987.

[52] G. P. A. Agrawal, “Intensity dependence of the linewidth enhancement factor and its implications for semiconductor lasers,” *IEEE Photon. Technol. Lett.*, vol. 1, no. 8, pp. 212–214, Aug. 1989.

[53] A. Villafranca *et al.*, “Linewidth enhancement factor of semiconductor lasers: Results from Round-Robin measurements in COST 288 action,” in *Proc. Opt. Soc. Amer. Conf. Lasers Electro-Opt.(CLEO)*, 2007.

[54] J. Provost and F. Grillot, “Measuring the chirp and the linewidth enhancement factor of optoelectronic devices with a Mach–Zehnder interferometer,” *IEEE Photon. J.*, vol. 3, no. 3, pp. 476–488, Jun. 2011.

[55] F. Grillot, B. Dagens, J. Provost, H. Su, and L. F. Lester, “Gain compression and above-threshold linewidth enhancement factor in 1.3-μm InAs–GaAs quantum-dot lasers,” *IEEE J. Quantum Electron.*, vol. 44, no. 10, pp. 946–951, Oct. 2008.

[56] E. K. Lau, L. J. Wong, and M. C. Wu, “Enhanced modulation characteristics of optical injection-locked lasers: A tutorial,” *IEEE J. Sel. Topics Quantum Electron.*, vol. 15, no. 3, pp. 618–633, May/Jun. 2009.

[57] P. Miska, J. Even, O. Dehaese, and X. Marie, “Carrier relaxation dynamics in InAs/InP quantum dots,” *Appl. Phys. Lett.*, vol. 92, no. 19, pp. 191103-1–191103-3, May 2008.

[58] C. Cornet *et al.*, “Time-resolved pump probe of 1.55 μm InAs/InP quantum dots under high resonant excitation,” *Appl. Phys. Lett.*, vol. 88, no. 17, pp. 171502-1–171502-3, Apr. 2006.

[59] C. Cornet *et al.*, “Quantitative investigations of optical absorption in InAs/InP (311)B quantum dots emitting at 1.55 μm wavelength,” *Appl. Phys. Lett.*, vol. 85, no. 23, pp. 5685–5687, Dec. 2004.

[60] Y. Wu, R. A. Suris, and L. V. Asryan, "Effect of internal optical loss on the modulation bandwidth of a quantum dot laser," *Appl. Phys. Lett.*, vol. 100, no. 13, pp. 131106-1–131106-4, 2012.

[61] K. Kamath, J. Phillips, H. Jiang, J. Singh, and P. Bhattacharya, "Small-signal modulation and differential gain of single-mode self-organized $In_{0.4}Ga_{0.6}As/GaAs$ quantum dot lasers," *Appl. Phys. Lett.*, vol. 70, no. 22, pp. 2952–2953, Jun. 2012.

[62] B. Lingnau, W. W. Chow, and K. Lüdge, "Amplitude-phase coupling and chirp in quantum-dot lasers: Influence of charge carrier scattering dynamics," *Opt. Exp.*, vol. 22, no. 5, pp. 4867–4879, 2014.

[63] S. Melnik, G. Huyet, and A. Uskov, "The linewidth enhancement factor α of quantum dot semiconductor lasers," *Opt. Exp.*, vol. 14, no. 7, pp. 2950–2955, 2006.

[64] M. Gioannini, A. Sevega, and I. Montrosset, "Simulations of differential gain and linewidth enhancement factor of quantum dot semiconductor lasers," *Opt. Quantum Electron.*, vol. 38, nos. 4–6, pp. 381–394, 2006.

[65] M. Gioannini and I. Montrosset, "Numerical analysis of the frequency chirp in quantum-dot semiconductor lasers," *IEEE J. Quantum Electron.*, vol. 43, no. 10, pp. 941–949, Oct. 2007.

[66] J. M. Garcie *et al.*, "Intermixing and shape changes during the formation of InAs Self-assembled quantum dots," *Appl. Phys. Lett.*, vol. 71, no. 14, pp. 2014–2016, Oct. 1997.

[67] T. Raz, D. Ritter, and G. Bahir, "Formation of InAs self-assembled quantum rings on InP," *Appl. Phys. Lett.*, vol. 82, no. 11, pp. 1706–1708, Mar. 2003.

[68] J. Even and S. Loualiche, "Exact analytical solutions describing quantum dot, ring and wire wavefunctions," *J. Phys. A, Math. General*, vol. 37, no. 27, pp. L289–L294, 2004.

[69] M. Ishida *et al.*, "Photon lifetime dependence of modulation efficiency and K factor in 1.3 μm self-assembled InAs/GaAs quantum-dot lasers: Impact of capture time and maximum modal gain on modulation bandwidth," *Appl. Phys. Lett.*, vol. 85, no. 18, pp. 4145–4147, Nov. 2004.

Cheng Wang was born in Tengzhou, China, in 1987. He received the M.S. degree in physical electronics from the Harbin Institute of Technology, Harbin, China, in 2011. He is currently pursuing the Ph.D. degree with the Department of Materials and Nanotechnology, National Institute of Applied Sciences of Rennes, Rennes, France. His main research activities include dynamics and nonlinear dynamics of advanced nanostructure lasers, such as quantum-dot laser and quantum cascade laser.

Benjamin Lingnau was born in Berlin, Germany in 1988. He received the B.Sc. and M.Sc. degrees in physics from the Technische Universität (TU) Berlin, Berlin, Germany, in 2009 and 2011, respectively. He is currently pursuing the Ph.D. degree with the Group of E. Schöll at TU Berlin. His current research interests include quantum-dot optical devices and nonlinear laser dynamics.

Kathy Lüdge was born in Berlin, Germany, in 1976. She is a Senior Scientist with the Institute of Theoretical Physics, Technische Universität (TU) Berlin, Berlin. She received the Diploma and Dr.rer.nat degrees in physics from the Department of Solid-State Physics, TU Berlin, in 2000 and 2003, respectively. From 2001 to 2002, she was a Visiting Scholar with the Department of Material Science, University of Minnesota, Minneapolis, MN, USA. She received the Habilitation (*venia legendi*) degree from TU Berlin in 2011. Her research interests include the modeling of semiconductor quantum-dot lasers, nonlinear laser dynamics, and control with optical feedback. She is the Editor of the book *Nonlinear Laser Dynamics - From Quantum Dots to Cryptography* (Wiley, 2011) as the 5th volume of *Reviews of Nonlinear Dynamics and Complexi*.

Jacky Even was born in Rennes, France, in 1964. He received the Ph.D. degree from the University of Paris VI, Paris, France, in 1992. He was a Research and Teaching Assistant with the University of Rennes I, Rennes, from 1992 to 1999. He has been a Full Professor of Optoelectronics with the Institut National des Sciences Appliquées, Rennes, since 1999. He was the Head of the Materials and Nanotechnology with the Department of Insa Rennes from 2006 to 2009, and the Director of Education of Insa Rennes from 2011 to 2012. He created the FOTON Laboratory Simulation Group in 1999. His main field of activity is the theoretical study of the electronic, optical, and nonlinear properties of semiconductor QW and QD structures, hybrid perovskite materials, and the simulation of optoelectronic and photovoltaic devices. He has authored and co-authored 160 papers and 150 contributions in international conferences.

Frédéric Grillot was born in Versailles, France, in 1974. He received the M.Sc. degree from the University of Dijon, Dijon, France, in 1999, the Ph.D. degree in electrical engineering from the University of Besançon, Besançon, France, in 2003, and the Research Habilitation degree in physics from the University of Paris VII Denis Diderot, Paris, France, in 2012. His doctoral research activities were conducted with the Department of Optical Component Research, AlcatelLucent Bell Labs, Boulogne-Billancourt, France, working on the effects of the optical feedback in near infrared semiconductor lasers, and the impact this phenomenon has on high-speed optical communication systems. From 2003 to 2004, he was with the Institut d'Electronique Fondamentale, University Paris-Sud, Orsay, France, where he focused on integrated optics modeling and Si-based passive devices for optical interconnects. From 2004 to 2012, he was with the Institut National des Sciences Appliquées, Rennes, France, as an Assistant Professor. From 2008 to 2009, he was a Visiting Professor with the University of New Mexico, Albuquerque, NM, USA, leading research in optoelectronics with the Center for High Technology Materials. Since 2012, he has been an Associate Professor with the Department of Communications and Electronic, Telecom Paristech (alias Ecole Nationale Supérieure des Télécommunications), Paris. He has authored and co-authored 57 journal papers, one book, two book chapters, and more than 150 contributions in international conferences and workshops. His current research interests include advanced laser diodes using new materials (quantum dots, carbon nanotubes, quantum cascade, and hybrid silicon lasers), nonlinear dynamics and optical chaos in semiconductor lasers systems, and microwave photonics applications, including photonic clocks and photonic analog-to-digital converters. He is an Associate Editor of *Optics Express* and a Senior Member of the International Society for Optics and Photonics and the IEEE Photonics Society.